

Enhancement of  $T_c$  and the re-entrant spin glass transition in  $\text{La}_{0.86}\text{Ca}_{0.14}\text{Mn}_{1-y}\text{Cr}_y\text{O}_3$  ( $y = 0, 0.1$  and  $0.2$ )

This article has been downloaded from IOPscience. Please scroll down to see the full text article.

2004 J. Phys.: Condens. Matter 16 3691

(<http://iopscience.iop.org/0953-8984/16/21/017>)

View [the table of contents for this issue](#), or go to the [journal homepage](#) for more

Download details:

IP Address: 129.252.86.83

The article was downloaded on 27/05/2010 at 14:57

Please note that [terms and conditions apply](#).

## Enhancement of $T_c$ and the re-entrant spin glass transition in $\text{La}_{0.86}\text{Ca}_{0.14}\text{Mn}_{1-y}\text{Cr}_y\text{O}_3$ ( $y = 0, 0.1$ and $0.2$ )

T Sudyoasuk<sup>1,2</sup>, R Suryanarayanan<sup>2,3</sup> and P Winotai<sup>1</sup>

<sup>1</sup> Department of Chemistry, Mahidol University, Rama VI Road, Bangkok 10400, Thailand

<sup>2</sup> Laboratoire de Physico-Chimie de l'Etat Solide, UMR8648, Bâtiment 414, Université Paris-Sud, 91405 Orsay, France

E-mail: ramanathan.suryan@lpces.u-psud.fr

Received 13 January 2004

Published 14 May 2004

Online at [stacks.iop.org/JPhysCM/16/3691](http://stacks.iop.org/JPhysCM/16/3691)

DOI: 10.1088/0953-8984/16/21/017

### Abstract

We report on structural, frequency dependent ac susceptibility, dc magnetization and magnetoresistance (MR) measurements on polycrystalline samples of  $\text{La}_{0.86}\text{Ca}_{0.14}\text{Mn}_{1-y}\text{Cr}_y\text{O}_3$  ( $y = 0, 0.1$  and  $0.2$ ) prepared by the sol-gel technique. For  $y = 0$ , a paramagnetic to ferromagnetic transition was observed at  $T_c = 185$  K. For  $y = 0.1$ , the value of  $T_c = 200$  K, an increase of 15 K, and for  $y = 0.2$ ,  $T_c = 195$  K, an increase of 10 K. The imaginary part of the ac susceptibility for all three samples shows a secondary transition at  $T_f < T_c$ . For  $y = 0$ , there is no definite law accounting for the frequency dependence of  $T_f$  and it is attributed to a transition arising out of a canted structure. However, in the cases of  $y = 0.1$  and  $0.2$ , the frequency dependence indicates the presence of a re-entrant spin glass transition at  $T_f$ . Although all three samples show a semiconducting behaviour between 300 and 5 K, a negative MR was observed corresponding to  $T_c$  and  $T_f$ . The value of MR decreased for the Cr substituted samples.

### 1. Introduction

The manganites  $\text{Ln}_{1-x}\text{D}_x\text{MnO}_3$  ( $\text{Ln} = \text{Bi}$ , rare earths;  $\text{D} = \text{Pb}$ ,  $\text{Ca}$ ,  $\text{Sr}$ ,  $\text{Ba}$ ) exhibit interesting physical properties such as a paramagnetic to ferromagnetic (PFM) transition, a semiconductor to metal transition (SMT), negative colossal magnetoresistance (CMR), charge ordering (CO) and an isotope effect and are being extensively investigated [1–4]. The divalent (D) substitution and the dependence both on the value of  $x$  and on the ionic radius of the rare earth introduce mixed valence of  $\text{Mn}^{3+}$  and  $\text{Mn}^{4+}$  in these compounds that results in the delocalization of  $e_g$  electrons and a parallel alignment of  $t_{2g}$  spins. This is the basis of the double-exchange

<sup>3</sup> Author to whom any correspondence should be addressed.

model which accounts for the occurrence of the paramagnetic to ferromagnetic (PM–FM) transition accompanied by a semiconductor to metal (SMT) transition [5]. However, this model is inadequate to explain other properties as pointed out by several authors [3, 4, 6–8]. In particular, recent experiments seem to indicate that for certain values of  $x$ , the ground state is not a homogeneous ferromagnetic metallic (FMM) state but consists of regions of FM and antiferromagnetic (AFM) clusters [9]. The phase separation model relies heavily on such observations [3, 4]. Among manganites, the magnetic and magnetotransport properties of the  $\text{La}_{1-x}\text{Ca}_x\text{MnO}_3$  compounds have been fairly well studied [1, 2]. A variety of magnetic transitions are observed as  $x$  increases from 0 to 1. Magnetization and neutron scattering data have been reported for single crystals of  $\text{La}_{1-x}\text{Ca}_x\text{MnO}_3$  for  $x = 0.1, 0.125$  and  $0.2$  [10]. We note, in particular, that the AFM state that was present for  $x = 0$  disappears for  $x = 0.1$ , resulting in a PM–FM transition at 138 K, but the sample remains semiconducting down to 5 K. In addition to the PM–FM transition, the sample shows a secondary transition at 112 K resulting from a canted spin structure as inferred from neutron measurements. The sample with  $x = 0.125$  shows similar features. The SMT sets in only for  $x = 0.2$  and the canted structure disappears. We note that no experimental data exist for  $x = 0.14$ , though one expects for this composition, from the phase diagram of Biotteau *et al* [10], a PM–FM transition accompanied by a canted structure at  $T$  not far from 100 K. We are interested here in studying the effect of Cr substitution on the magnetic and magnetotransport properties of this lightly hole doped compound. Among the 3d elements, Cr substitution is particularly interesting as  $\text{Cr}^{3+}$  is isoelectronic with  $\text{Mn}^{4+}$  and is a non-Jahn–Teller ion. In addition, the nature of the magnetic  $\text{Cr}^{3+}\text{–O–Mn}^{3+}$  interaction is known to favour ferromagnetism through superexchange interaction. Several interesting properties have indeed been reported in relation to the effect of Cr substitution at the Mn sites of the perovskite manganites. Raveau *et al* [11] showed that 5% of Cr substituted on the Mn site in  $\text{Pr}_{0.5}\text{Ca}_{0.5}\text{MnO}_3$  not only completely suppressed the CO transition but also induced a PM–FM transition that was accompanied by a semiconductor to metal transition and the sample showed a CMR in the presence of a moderate magnetic field. In the case of  $\text{La}_{0.46}\text{Sr}_{0.54}\text{Mn}_{1-y}\text{Cr}_y\text{MnO}_3$ , a re-entrant spin glass behaviour was observed for  $y = 0.02$  [12]. In the case of electron doped compounds such as  $\text{La}_{0.7}\text{Ca}_{0.3}\text{Mn}_{1-y}\text{Cr}_y\text{MnO}_3$ , the CO that was observed for  $y = 0$  at 260 K was completely suppressed in the  $y = 0.2$  sample and, though no SMT was observed, a sizable CMR was reported due to spin dependent hopping [13]. In another electron doped manganite system,  $\text{Sm}_{1-x}\text{Ca}_x\text{MnO}_3$ , the substitution of Ni, Co and Cr at the Mn sites resulted in the disappearance of the CO, and a CMR effect and a ferromagnetic semi-metallic ground state were observed [14–16]. With these features in mind, we have carried out structural, frequency dependent ac susceptibility, dc magnetization and magnetoresistance measurements on the polycrystalline samples of  $\text{La}_{1-x}\text{Ca}_x\text{Mn}_{1-y}\text{Cr}_y\text{O}_3$  ( $y = 0, 0.1$  and  $0.2$ ) prepared by the sol–gel technique.

## 2. Experimental details

The polycrystalline samples reported on here were prepared by the well known sol–gel technique. Stoichiometric amounts of  $\text{La}(\text{NO}_3)_3 \cdot 6\text{H}_2\text{O}$  (99%),  $\text{CaCO}_3$  (99.5%),  $\text{Cr}(\text{NO}_3)_3 \cdot 9\text{H}_2\text{O}$  (97%) and  $\text{Mn}(\text{CH}_3\text{COO})_2 \cdot 4\text{H}_2\text{O}$  (99%) were dissolved in a dilute  $\text{HNO}_3$  solution with citric acid and ethylene glycol used as the chelating agents. The mixed solution was then heated until a dark coloured resin material was formed. The resin was subsequently fired at 773 and 1173 K in air to decompose the organic residual. The resultant powder was then ground, pelletized and sintered at 1573 K for 12 h.

Room temperature powder x-ray diffraction (XRD) measurements on these samples were carried out with a Bruker D8 advanced diffractometer in the Bragg–Brentano geometry using

**Table 1.** Lattice parameters for  $\text{La}_{0.86}\text{Ca}_{0.14}\text{MnO}_3$ ,  $\text{La}_{0.86}\text{Ca}_{0.14}\text{Mn}_{0.90}\text{Cr}_{0.10}\text{O}_3$  and  $\text{La}_{0.86}\text{Ca}_{0.14}\text{Mn}_{0.80}\text{Cr}_{0.20}\text{O}_3$  from the Rietveld refinement of x-ray diffraction data. The numbers in parentheses are estimated standard deviations to the last significant digit and  $\sigma_{\text{JT}}^2 = 1/6 \sum \{[d_{(\text{Mn}-\text{O})_i} - d_{(\text{Mn}-\text{O})}] / d_{(\text{Mn}-\text{O})}\}^2$ .

	$\text{La}_{0.86}\text{Ca}_{0.14}\text{MnO}_3$	$\text{La}_{0.86}\text{Ca}_{0.14}\text{Mn}_{0.90}\text{Cr}_{0.10}\text{O}_3$	$\text{La}_{0.86}\text{Ca}_{0.14}\text{Mn}_{0.80}\text{Cr}_{0.20}\text{O}_3$
$a$ (Å)	5.4959(1)	5.4987(1)	5.4858(1)
$b$ (Å)	5.5040(1)	5.5116(1)	5.5057(1)
$c$ (Å)	7.7920(1)	7.7713(2)	7.7619(2)
$V$ (Å <sup>3</sup> )	235.70(1)	235.52(1)	234.43(1)
$\langle d_{\text{Mn}-\text{O}} \rangle$	1.975	1.967	1.964
$\theta_{(\text{Mn}-\text{O}-\text{Mn})}$ (deg)	160.12 (deg)	164.04 (deg)	164.81 (deg)
$\sigma_{\text{JT}}^2$	$1.27 \times 10^{-5}$	$1.53 \times 10^{-5}$	$2.92 \times 10^{-4}$

Cu  $K\alpha$  radiation. The XRD patterns were recorded from  $2\theta = 20^\circ$  to  $130^\circ$  with a  $0.02^\circ$  step size and a counting time of 12 s. Further analysis by the Rietveld method using the *FULLPROF* program was carried out [17]. The surface morphology and composition of the samples were examined using a scanning electron microscope (SEM) fitted with an energy dispersive spectrometer. The SEM micrographs showed a granular structure for all three samples with a highly dense morphology with little or no porosity and typical grain sizes on the order of  $1 \mu\text{m}$ . The energy dispersive x-ray analysis indicated that the composition of the cations was quite close to the nominal one. Both the real ( $\chi'$ ) and imaginary ( $\chi''$ ) parts of the ac susceptibility of the samples were measured as a function of temperature using a home built apparatus in which one could vary the frequency of the ac exciting field from 40 to 18 000 Hz. The dc magnetization as a function of temperature and magnetic field was measured using a commercial SQUID magnetometer. Resistance was measured as a function of temperature and in zero and in an applied field of 5 T using a special sample holder that could be inserted into the cryostat of the SQUID magnetometer. Silver paint was used to make electrical contacts and the standard four-point technique was used for these measurements.

### 3. Results

#### 3.1. XRD data

The XRD pattern for the three samples is shown in figure 1. Neither the presence of any impurity phases nor that of any precipitates of unreacted oxides could be detected. These patterns could be indexed to the  $\text{GdFeO}_3$  perovskite structure with the space group *Pbnm*. The calculated lattice parameters and other details are tabulated in table 1. The unit cell volume and the average distance  $\langle d_{\text{Mn}-\text{O}} \rangle$  of the sample decrease as a function of Cr content. There is a general tendency for the angle  $\theta_{(\text{Mn}-\text{O}-\text{Mn})}$  to increase as the Cr content increases, though this increase is more notable for the  $y = 0.1$  sample. The distortion of the  $\text{MnO}_6$  octahedra in the 0.2 Cr doped sample ( $\sigma_{\text{JT}}^2 = 2.92 \times 10^{-4}$ ) is much higher than that of the parent sample ( $\sigma_{\text{JT}}^2 = 1.27 \times 10^{-5}$ ).

#### 3.2. The ac susceptibility

The real and the imaginary parts of the ac susceptibility of the samples as a function of temperature measured in an ac excitation field of 5.5 Oe with a frequency set at 1.5 kHz are shown in figures 2(a)–(c). Several interesting features can be noticed. For  $y(\text{Cr}) = 0$ ,  $\chi'$  rises abruptly as  $T$  approaches 190 K, indicative of a paramagnetic to ferromagnetic transition

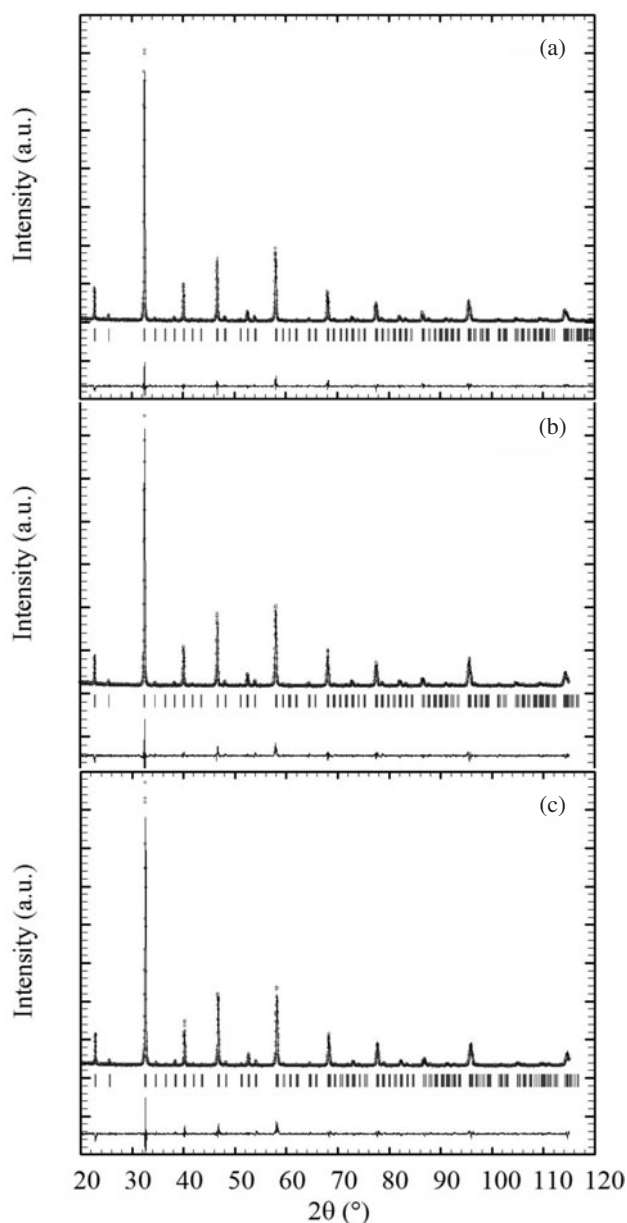


**Figure 1.** X-ray diffraction spectra of (a)  $\text{La}_{0.86}\text{Ca}_{0.14}\text{MnO}_3$ , (b)  $\text{La}_{0.86}\text{Ca}_{0.14}\text{Mn}_{0.9}\text{Cr}_{0.1}\text{O}_3$  and (c)  $\text{La}_{0.86}\text{Ca}_{0.14}\text{Mn}_{0.8}\text{Cr}_{0.2}\text{O}_3$ . Data points are indicated with solid circles, while the calculated patterns are shown as a continuous line. The positions of the reflections are indicated with the vertical lines below the patterns.

(PM–FM), shows a small peak at 173 K and decreases slowly with a broad maximum around 120 K. On the other hand,  $\chi''$  shows a step-like feature at ( $T_c$ ) 185 K and rapidly increases with a flat region between 150 and 125 K followed by a somewhat broad maximum centred at ( $T_f$ ) 95 K. For  $y(\text{Cr}) = 0.1$ , there is a remarkable increase in the  $\chi'$  peak from 173 to 189 K and the intensity decreases around 115 K. The step-like feature in  $\chi''$  is also seen to occur at

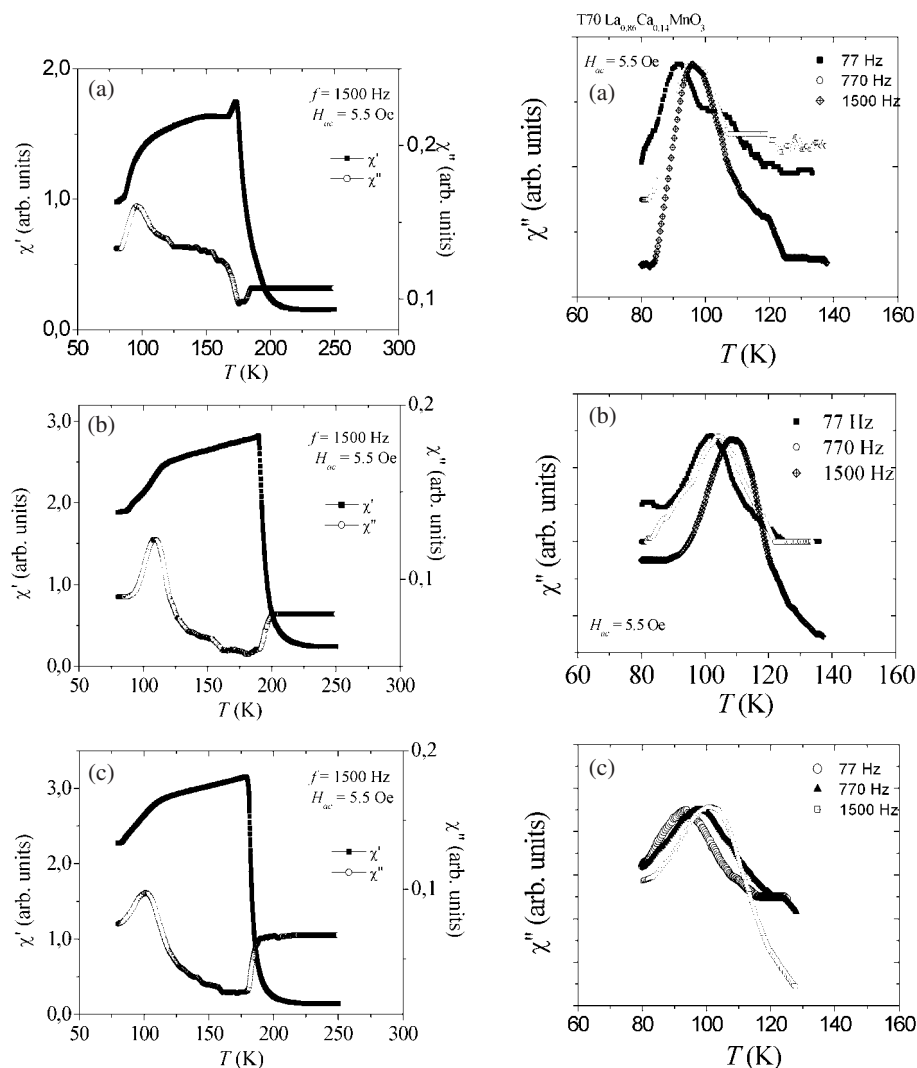


**Figure 2.** Real ( $\chi'$ ) and imaginary ( $\chi''$ ) parts of the ac susceptibility of  $\text{La}_{0.86}\text{Ca}_{0.14}\text{Mn}_{1-y}\text{Cr}_y\text{O}_3$  as a function of temperature. (a)  $y = 0$ ; (b)  $y = 0.1$ ; (c)  $y = 0.2$ .

**Figure 3.** The imaginary part ( $\chi''$ ) of the ac susceptibility of  $\text{La}_{0.86}\text{Ca}_{0.14}\text{Mn}_{1-y}\text{Cr}_y\text{O}_3$  as a function of temperature at three different frequencies. (a)  $y = 0$ ; (b)  $y = 0.1$ ; (c)  $y = 0.2$ .

a higher temperature (200 K) indicating a net increase of about 15 K in  $T_c$ . The maximum in  $\chi''$  also shifts to a higher temperature of  $T_f = 108$  K and the flat region seen in the case of  $y = 0$  is somewhat suppressed indicating a change in magnetic structure in the region below 150 K. For a further increase in the Cr concentration to  $y = 0.2$ , both the peak in  $\chi'$  and the step-like feature in  $\chi''$  shift to lower temperatures—respectively to 180 and 195 K—and the second maximum in  $\chi''$  broadens; it is centred at 100 K. With respect to  $y = 0$ , there is a net increase in  $T_c$  of 10 K and, further, the flat region below 150 K resembles that observed in the case of  $y = 0.1$ .

We next demonstrate the effect of the ac frequency of the exciting field on the imaginary part of the ac susceptibility for these samples. Though the low temperature part of  $\chi'$  was

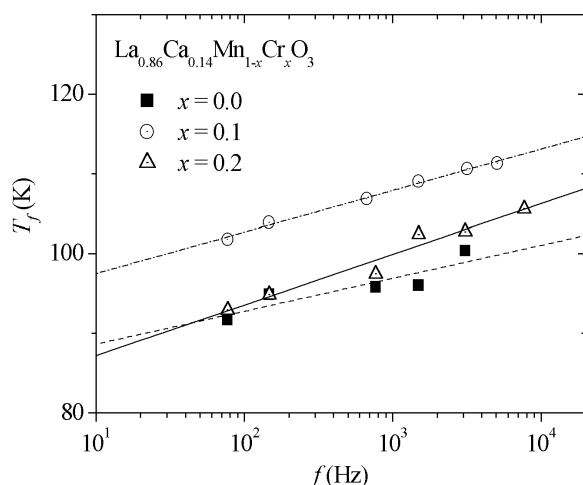


**Figure 4.**  $T_f$  for  $\text{La}_{0.86}\text{Ca}_{0.14}\text{Mn}_{1-y}\text{Cr}_y\text{O}_3$  ( $y = 0.1$  and  $0.2$ ) as a function of frequency ( $f$ ).

affected by the change in frequency ( $f$ ), it is the low temperature part of  $\chi''$  (showing a fairly well defined maximum) that exhibits easily measurable shifts. As typical examples, figures 3(a)–(c) show the data at three different frequencies. The value of  $T_f$  shifted to higher temperature as the frequency of the measurement increased. This phenomenon is characteristic of spin glasses [18]. To understand the nature of this transition, we have plotted  $T_f$  as a function of  $f$  (figure 4). A straight line fit is obtained only in the case of Cr substituted samples indicating that a different mechanism is involved in the case of the parent compound ( $y = 0$ ). In the case of  $y = 0.1$  and  $0.2$ , we have determined the freezing temperature ( $T_g$ ) by extrapolating the curve to zero frequency. Taking the experimental values of  $T_f$  and the extrapolated value of  $T_g$  for these two samples, we have used the conventional spin glass formula for critical slowing down to analyse our data (figure 5). According to this model [18]

$$\tau/\tau_0 = [(T_f - T_g)/T_g]^{-z\nu}. \quad (1)$$

Here,  $T_g$  is the spin glass transition temperature and  $T_f$  is the frequency dependent freezing temperature at which the maximum relaxation time  $\tau$  corresponds to the measured frequency,  $\tau_0$  is the characteristic time constant of the spin glass and  $z\nu$  is a critical component. The data for  $y = 0.1$  and  $0.2$  satisfy this relation yielding respectively  $\tau_0 = 2.89 \times 10^{-9}$  s and  $1.78 \times 10^{-8}$  s and  $z\nu = 6.05$  and  $6.17$  (figure 5).

### 3.3. The dc magnetization

The magnetization ( $M$ ) of the three samples at 6 K, as a function of magnetic field, is shown in figure 6. The magnetizations of all the samples are saturated at relatively low fields and the values of the saturated magnetic moment for  $y = 0, 0.1$  and  $0.2$  are respectively  $3.72, 3.09$  and  $2.41 \mu_B/\text{fu}$ . The zero-field cooled (zfc) and field cooled (fc) magnetizations measured in a field of  $0.005$  T, as a function of temperature, are shown in figures 7(a)–(c). The data show clearly that the substitution of Cr enhances the value of  $T_c$ . Further, for all the samples, there is a difference between zfc and fc data. This may be indicative of spin glass like behaviour or merely indicate irreversible effects which can be due to irreversible domain wall dynamics. The difference between zfc and fc data at low temperatures decreases as a function of Cr substitution indicating a modification of the magnetic structure. This difference almost vanishes for  $H = 1$  T for all three samples. We have also tried to fit the high temperature ( $200 < T < 300$  K) magnetization data to a Curie–Weiss law (not shown here). The data

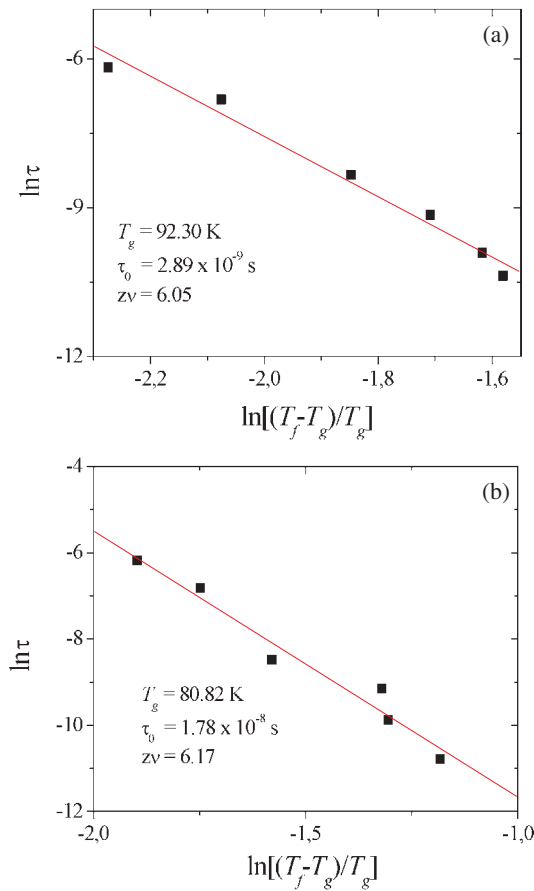


**Figure 5.**  $\ln \tau$  as a function of  $\ln[(T_f - T_g)/T_g]$ . (a)  $y = 0$ ; (b)  $y = 0.2$ .

(This figure is in colour only in the electronic version)

yielded a positive intercept at 194, 215 and 198 K respectively for  $y = 0, 0.1$  and  $0.2$  and the respective moments ( $H = 0.005$  T)  $p_{\text{eff}}$  were 6.18, 5.32 and  $4.5 \mu_B$ . The values of  $p_{\text{eff}}$  were found to depend on the applied magnetic field and in general increased with the field. Thus, these values for the three samples were 6.53 and  $6.63 \mu_B$ ; 5.54 and  $5.67 \mu_B$ ; 4.78 and  $5.02 \mu_B$  when the applied field was 0.05 and 1 T respectively.

### 3.4. Resistivity and magnetoresistance

The resistivities ( $\rho$ ) of the three samples, as a function of temperature in zero ( $\rho_0$ ) and 5 T ( $\rho_H$ ), are shown in figure 8. All three samples show semiconducting behaviour in zero field. The data show a small change in slope at temperatures corresponding to  $T_c$ ; though the samples remain semiconductors in an applied field of 5 T, the change in slope is suppressed and the resistivity decreases especially for the samples with  $y = 0$  and  $0.1$ . The magnetoresistance ( $\text{MR}\% = -100 \times (\rho_H - \rho_0)/\rho_0$ ) shown as a function of temperature in figure 9 reveals interesting features. For all three samples, a non-zero MR is observed close to 300 K which is much higher than  $T_c$ . For  $y = 0$ , the MR increases rapidly from near 300 K reaching values greater than 50% and shows two distinct maxima at 180 and at 100 K. The high resistivity for  $T < 50$  K prevented us from obtaining reliable data on MR, though MR showed an increase for  $T > 75$  K. For  $y = 0.1$ , the value of MR reduced to 30% but a distinct maximum in MR



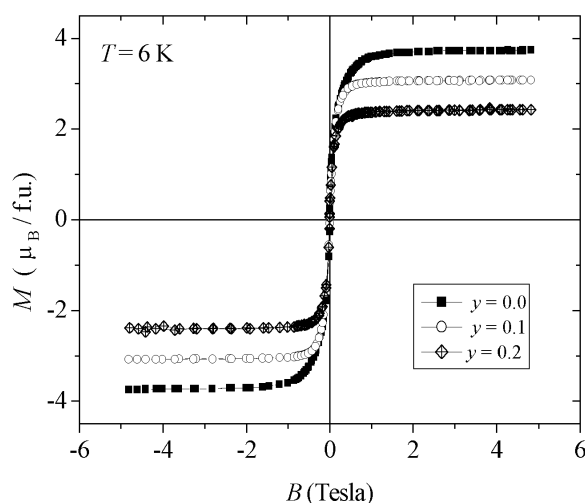


**Figure 6.** Magnetization at 6 K of  $\text{La}_{0.86}\text{Ca}_{0.14}\text{Mn}_{1-y}\text{Cr}_y\text{O}_3$  ( $y = 0, 0.1$  and  $0.2$ ) as a function of field.

was observed at 200 K followed by a broad maximum centred at 125 K. For  $y = 0.2$ , the value of MR was further reduced to about 20% and only a broad maximum centred at around 160 K was observed.

#### 4. Discussion

It is well known that in the manganites,  $\text{Ln}_{1-x}\text{D}_x\text{MnO}_3$ , there is a strong competition between superexchange and double-exchange interactions. This leads to a variety of magnetic orderings depending on the ionic radii of Ln and D and the value of  $x$ . The samples of interest to us are in the lightly hole doped region of the phase diagram of  $\text{La}_{1-x}\text{Ca}_x\text{MnO}_3$ . Though Biotteau *et al* [10] have not reported any data for  $x = 0.14$ , the composition of interest to us, it is reasonable to extrapolate the properties from the published phase diagram. Thus, one would expect the sample with  $x = 0.14$  to show a PM–FM transition followed by another transition with a canted structure similar to that reported for  $x = 0.1$  and  $0.125$ . Our ac susceptibility data do indeed indicate a PM–FM transition at  $T_c \approx 185$  K with another secondary transition at a lower temperature  $T_f = 95$  K. The frequency response of this secondary transition does not provide a good fit with equation (1) to identify it with a conventional spin glass. One may attribute this to a canted structure similar to that observed for  $x = 0.125$  by Biotteau *et al* [10] though neutron scattering experiments would have to be carried out to ascertain this. Following Dagotto *et al* [4], this transition may arise from spin cluster glass, an antiferromagnetic matrix containing ferromagnetic clusters, that can give rise to a magnetoresistance effect as was indeed observed in our sample. As pointed out by Dagotto [19], the exact nature of these spin clusters as regards the classical spin glass is not clear at the present moment and is currently under investigation by several others. We wish to add further that the sample with  $x = 0$ , reported to exhibit a canted spin structure by Biotteau *et al* [10], was re-examined by Yates *et al* [20] using NMR techniques. Their data do not rule out the possibility that the ferromagnetic host is canted but certainly do not support this for true long range phase coexistence, thus indicating the complexity of the properties of these materials.

The substitution of Cr leads to three noticeable effects—an increase in  $T_c$ , a re-entrant spin glass transition at lower temperatures and a suppression of the CMR. The increase in  $T_c$  can be related to the increase in the FM exchange interaction between  $\text{Mn}^{3+}$  and  $\text{Cr}^{3+}$ , which can be

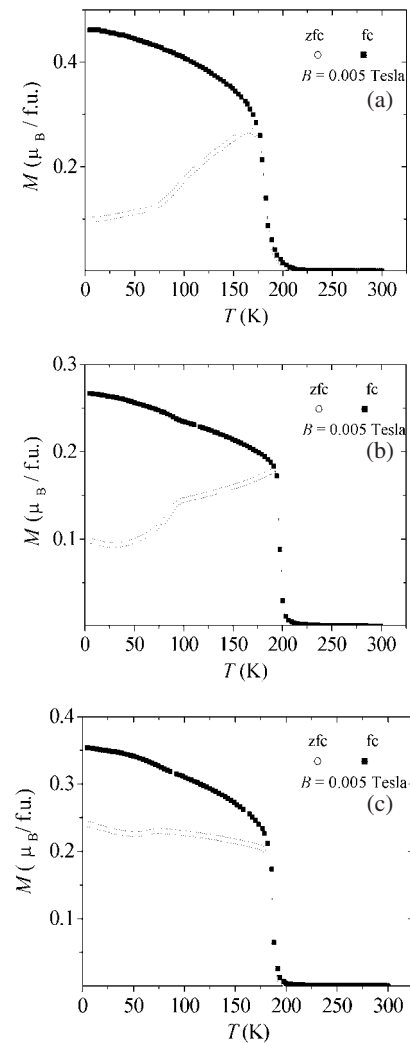


**Figure 7.** Magnetization of  $\text{La}_{0.86}\text{Ca}_{0.14}\text{Mn}_{1-y}\text{Cr}_y\text{O}_3$  as a function of temperature. (a)  $y = 0$ ; (b)  $y = 0.1$ ; (c)  $y = 0.2$ .

inferred from the increase in the paramagnetic Curie–Weiss temperature, and also to the change in structural parameters such as  $\theta_{(\text{Mn}-\text{O}-\text{Mn})}$ . The presence of  $\text{Cr}^{3+}$  effectively contributes to an increase in  $\text{Mn}^{4+}$  content and can account for the reduction in the saturated magnetic moment. On the other hand, the high value of the  $p_{\text{eff}}$  compared to the theoretically expected value and the dependence on the magnetic field is attributed to the presence of magnetic polarons. Such a behaviour was also observed by Martinez *et al* [21] in the case of  $\text{La}_{0.9}\text{Ca}_{0.1}\text{MnO}_3$ .  $p_{\text{eff}}$  for a single crystal of this composition increased from 4.8 to 5.8  $\mu_{\text{B}}/\text{fu}$  when the measured field was increased from  $2.5 \times 10^{-4}$  to 5 T.

The transitions ( $\chi''$ ) observed at  $T_f$  for the  $y = 0.1$  and 0.2 samples exhibit a frequency dependence that is well known in the case of a spin glass. In the case of a conventional spin glass one observes  $\tau_0 = 10^{-13}$  s whereas the value obtained here is somewhat larger,  $10^{-10}$  s. Such a difference may be attributed to the presence of ferromagnetic clusters. Several others have observed either re-entrant spin glass behaviour or a spin glass transition in manganites and cobaltates. We will present a short discussion of a few cases that are

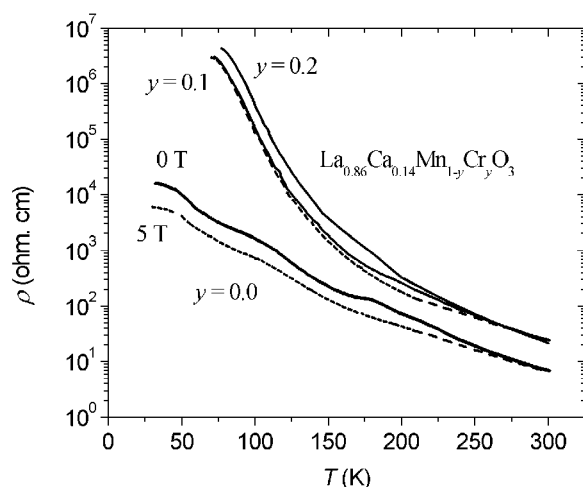


**Figure 8.** Resistivity (in  $H = 0$  and  $5$  T) of  $\text{La}_{0.86}\text{Ca}_{0.14}\text{Mn}_{1-y}\text{Cr}_y\text{O}_3$  ( $y = 0, 0.1$  and  $0.2$ ) as a function of temperature. The data for the sample with  $y = 0.2$  in  $H = 5$  T cannot be seen on the log scale because of a small magnetoresistance effect.

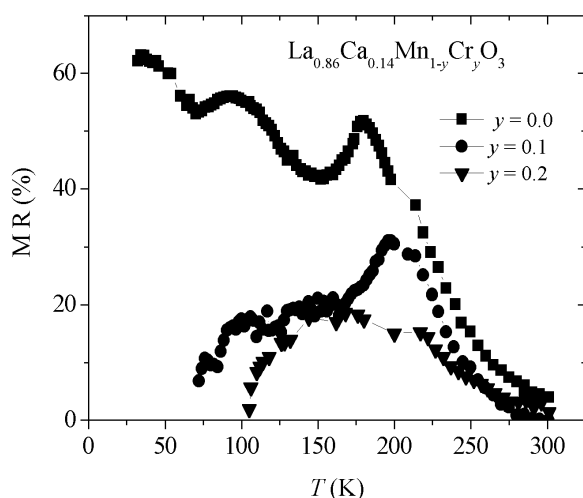


**Figure 9.** Magnetoresistance (see the text for a definition) in a field of  $5$  T of  $\text{La}_{0.86}\text{Ca}_{0.14}\text{Mn}_{1-y}\text{Cr}_y\text{O}_3$  ( $y = 0, 0.1$  and  $0.2$ ) as a function of temperature.

relevant to the present study. Studies on manganites exhibiting spin glass behaviour display varying degrees of magnetoresistance ranging from a CMR in  $(\text{La}_{1/3}\text{Tb}_{2/3})_{2/3}\text{Ca}_{1/3}\text{MnO}_3$  as a result of a field induced semiconductor–metal transition for fields greater than  $5$  T [22] to no magnetoresistance effect in  $\text{Y}_{0.5}\text{Sr}_{0.5}\text{MnO}_3$  for fields as high as  $4$  T [23]. The compound  $\text{La}_{0.46}\text{Sr}_{0.56}\text{Mn}_{1-y}\text{Cr}_y\text{O}_3$  shows a PM to FM and FM to AFM transitions at  $272$  and  $190$  K respectively [12]. For  $y = 0.02$ , in addition to the AFM transition, these authors observed a re-entrant spin glass transition at lower temperatures and their data follow equation (1), yielding a value of  $\tau_0 = 10^{-13}$  s. However, no CMR data were reported. In the case of the compound  $\text{La}_{0.95}\text{Sr}_{0.05}\text{CoO}_3$ , only one magnetic transition was identified at  $15$  K which showed a frequency dependent ac susceptibility yielding a value of  $\tau_0 = 2.3 \times 10^{-10}$  s [24]. Maignan *et al* [25] examined the magnetic properties of the compounds  $\text{Th}_{0.35}\text{D}_{0.65}\text{MnO}_3$  and showed the role played by the ionic size of D in the appearance of a spin glass insulating state.

Another interesting system is  $\text{La}_{0.96-z}\text{Nd}_z\text{K}_{0.04}\text{MnO}_3$  in which a disordered magnetic state is formed as La is replaced by Nd( $z$ ), reflecting the competition between FM double-exchange and AFM superexchange interactions [26]. In particular, for  $z = 0.4$ , a re-entrant spin glass

transition was reported at  $T_f$  ( $T_f < T_c$ ) and further in a field of 5 T a second maximum in the MR was noticed corresponding to a value of  $T_f$  quite similar to that we report here. In our case, for  $y = 0$ , the system is already in a disordered state as indicated by an additional transition (attributed to a canted structure) at  $T_f$  ( $T_f < T_c$ ). A moderate field of 5 T is able to reduce the spin disorder scattering resulting in an MR effect centred at  $T_f$ . The substitution of Cr further causes a change in the magnetic structure near  $T_f$  resulting in an increased frustration. This would increase the zero-field resistivity at low temperatures and reduce the MR effect as observed. On the other hand, the  $MR > 0$  for  $T > T_c$ , which may be attributed to the presence of magnetic polarons, as was also suggested by Martinez *et al* [21] in the case of  $\text{La}_{0.9}\text{Ca}_{0.1}\text{MnO}_3$ .

We also need to consider other points such as (a) the impact of charge ordering and its stability under Cr doping and (b) orbital ordering. For example, for compositions  $x > 0.14$ , Dai *et al* [27] have pointed out that charge ordering becomes short range. And Kimura *et al* [28] have shown that charge ordering can be destroyed to give a ferromagnetic ordering by Cr doping. Hence, to account for the increase in  $T_c$ , one might propose that an additional contribution may arise from such a destruction of charge ordering even on a local scale. Regarding point (b), one may note that with various dopings, orbital ordering can be frustrated to produce a Jahn–Teller glass, that is a frustrated glassy like arrangement of  $e_g$  orbitals. In fact, in  $\text{Pr}_{0.7}\text{Ca}_{0.3}\text{MnO}_3$ , such states were shown to behave like a spin glass [29].

We would like to conclude this section by commenting briefly on two models that are relevant to the present work. The first one is the phase separation model [3, 4] according to which the competition between AFM and FM states leads to inhomogeneities, especially in the case of lightly doped manganites, resulting in phase segregation. This phase segregated state may have some similarities to the classical spin glass similar to what we have reported here. An increased presence of the AFM component does not lead to the metallic state in zero magnetic field but a moderate field would enhance the tunnelling due to field induced alignment of magnetic domains resulting in a negative MR. The second, recent, model considers three strong on-site interactions, namely Jahn–Teller (JT) coupling which splits the twofold  $e_g$  orbital degeneracy, Hund’s coupling and  $e_g$  electron repulsion [8]. The new approach taken by these authors is considering the coexistence of JT polarons (l band) and the broad band of  $e_g$  states (b band). According to these authors, the effective bandwidth  $2D$  of the b electrons decreases (for small Ca concentration) and the b band bottom is above the l level. This leads to a low temperature insulating state. Further, the sample exhibits a PM–FM transition because of strong nearest neighbour exchange between  $t_{2g}$  spins as is indeed observed in the present study. However, the details of a further canted or spin glass like structure below  $T_c$  have not been worked out yet in this model.

## 5. Conclusions

We have carried out structural, frequency dependent ac susceptibility, dc magnetization and magnetoresistance (MR) measurements on polycrystalline samples of  $\text{La}_{0.86}\text{Ca}_{0.14}\text{Mn}_{1-y}\text{Cr}_y\text{O}_3$  ( $y = 0, 0.1$  and  $0.2$ ) prepared by the sol–gel technique. For  $y = 0$ , a paramagnetic to ferromagnetic transition was observed at  $T_c = 185$  K. The Cr substitution increases the value of  $T_c$  to 200 K for  $y = 0.1$  and to 195 K for  $y = 0.2$ . The imaginary part of the ac susceptibility shows a secondary transition at  $T_f < T_c$  for  $y = 0$ , which is attributed to a transition arising out of a canted structure. However, in the case of  $y = 0.1$  and  $0.2$ , the frequency dependence indicates the presence of a re-entrant spin glass transition at  $T_f$ . Though all three samples show no semiconductor to metal transition between 300 and 5 K, a negative MR was observed corresponding to  $T_c$  and  $T_f$ . The value of MR decreased for the Cr substi-

tuted samples. Since the spin glass phase observed here giving rise to a CMR effect might have some similarities with the phase segregated states evoked in certain models [3, 4, 19], we believe that the present work would be of considerable significance.

### Acknowledgments

TS, PW and RS thank the Thai Royal Golden Jubilee programme for financial support and PERCH for partial financial support. TS wishes to thank A Revcolevschi for hospitality shown to him during his stay in Orsay.

### References

- [1] Rao C N R and Raveau B (ed) 1998 *Colossal Magnetoresistance, Charge Ordering and Related Properties of Manganese Oxides* (Singapore: World Scientific)
- [2] Tokura Y (ed) 2000 *Colossal Magnetoresistive Oxides* (New York: Gordon and Breach)
- [3] Nagaev E L 2002 *Colossal Magnetoresistance and Phase Separation in Magnetic Semiconductors* (London: Imperial College Press)
- [4] Dagotto E, Hotta T and Moreo A 2001 *Phys. Rep.* **344** 1
- [5] Zener C 1951 *Phys. Rev.* **82** 403
- [6] Millis A J, Shraiman B I and Littlewood P B 1995 *Phys. Rev. Lett.* **74** 5144
- [7] Millis A J, Shraiman B I and Mueller R 1996 *Phys. Rev. B* **54** 5389
- [8] Venkateswara Pai G, Hassan S R, Krishnamurthy H R and Ramakrishnan T V 2003 *Europhys. Lett.* **64** 696  
Ramakrishnan T V, Krishnamurthy H R, Hassan S R and Venkateswara Pai G 2003 *Colossal Magnetoresistive Manganites* ed T Chatterji (Dordrecht: Kluwer–Academic) (Preprint cond-mat/038376)
- [9] Fäth M, Freisem S, Menovsky A A, Tomioka Y, Arts J and Mydosh J A 1999 *Science* **285** 1540  
Uehara M, Mori S, Chen C H and Cheong S W 1999 *Nature* **399** 560
- [10] Biotteau G, Hennion M, Mossa F, Rodriguez-Carvajal J, Pinsard L and Revcolevschi A 2001 *Phys. Rev. B* **64** 104421
- [11] Raveau B, Maignan A and Martin C 1997 *J. Solid State Chem.* **130** 162
- [12] Dho J, Kim W S and Hor N H 2002 *Phys. Rev. Lett.* **89** 027202
- [13] Sudadyosuk T, Suryanarayanan R and Winotai P 2004 *J. Magn. Magn. Mater.* at press
- [14] Damay F, Martin C, Maignan A and Raveau B 1998 *J. Magn. Magn. Mater.* **183** 143
- [15] Maignan A, Martin C, Damay F, Hervieu M and Raveau B 1998 *J. Magn. Magn. Mater.* **188** 185
- [16] Maignan A, Martin C and Raveau B 1999 *Mater. Res. Bull.* **34** 345
- [17] Rodriguez-Carvajal J 1993 *Physica B* **192** 55
- [18] Mydosh J A 1993 *Spin Glasses—An Introduction* (London: Taylor and Francis)
- [19] Dagotto E 2002 *Nanoscale Phase Separation and Colossal Magnetoresistance* (Berlin: Springer) chapter 16
- [20] Yates K A, Kapusta C, Riedi P C, Ghivelder L and Cohen L F 2003 *J. Magn. Magn. Mater.* **260** 105
- [21] Martinez B, Laukhin V, Fontcuberta J, Pinsard L and Revcolevschi A 2002 *Phys. Rev. B* **66** 054436
- [22] de Teresa M D, Ibarra M R, García J, Blasco J, Ritter C, Algarabel P A, Marquina C and del Moral A 1996 *Phys. Rev. Lett.* **76** 3392
- [23] Chatterjee S and Nigam A K 2002 *Phys. Rev. B* **66** 104403
- [24] Nam D N H, Mathieu R, Nordblad R, Khiem N V and Phuc N X 2000 *Phys. Rev. B* **62** 8989
- [25] Maignan A, Martin C, Van Tendeloo G, Hervieu M and Raveau B 1999 *Phys. Rev. B* **60** 15214
- [26] Mathieu R, Svendlindh P and Nordblad P 2000 *Europhys. Lett.* **52** 441
- [27] Dai P, Fernandez-Baca J A, Wakabayashi N, Plumer E W, Tomioka Y and Tokura Y 2000 *Phys. Rev. Lett.* **85** 2553
- [28] Kimura T, Kumai R, Okimoto Y, Tomioka Y and Tokura Y 2000 *Phys. Rev. B* **62** 15021
- [29] Radaelli P G, Ibarra R M, Argyriou D N, Casalta H, Andersen K M, Cheong S W and Mitchell J F 2001 *Phys. Rev. B* **63** 172419